



## Numerical analysis of TRIGA mark II reactor through Serpent code

COURSE OF ‘EXPERIMENTAL NUCLEAR REACTOR KINETICS’ - MSc. OF NUCLEAR ENGINEERING

Musile Tanzi Marco

**Professors:**  
Lorenzi Stefano

**Academic year:**  
2023-2024

**Abstract:** This is the report for the 2023-2024 course of ‘*Experimental Nuclear Reactor Kinetics*’. The objective was to develop a comprehensive 3-D Monte Carlo model through Serpent code to simulate the neutronic behavior inside the first configuration of the TRIGA mark II reactor in Pavia. The work then proceeded by assessing several key parameters and comparing them with the ones obtained experimentally, to check the validity of the model. The script used for the analysis can be found at the following link: [TRIGA Serpent code](#).

**Key-words:** TRIGA, Serpent, group constants, beta effective, reactivity coefficient.

## Contents

|  |           |
|--|-----------|
| <b>1 TRIGA description</b>                                   | <b>2</b>  |
| <b>2 Objective</b>   | <b>2</b>  |
| <b>3 Monte Carlo method and Serpent code</b>                 | <b>3</b>  |
| <b>4 Model</b>   | <b>3</b>  |
| <b>5 Results</b>   | <b>5</b>  |
| 5.1 Neutron flux spectrum . . . . .                          | 5         |
| 5.2 Diffusion homogenized group constants . . . . .          | 7         |
| 5.2.1 Two-group diffusion coefficients . . . . .             | 7         |
| 5.2.2 Two-group macroscopic cross sections . . . . .         | 7         |
| <b>6 Comparison with experimental results</b>                | <b>8</b>  |
| 6.1 Effective delayed neutron fraction . . . . .             | 8         |
| 6.2 REG control rod worth . . . . .                          | 9         |
| 6.3 REG calibration curve . . . . .                          | 10        |
| 6.4 Fuel temperature prompt reactivity coefficient . . . . . | 11        |
| 6.5 Void reactivity coefficient . . . . .                    | 11        |
| <b>7 Conclusion</b>  | <b>12</b> |

## 1. TRIGA description

The TRIGA (Training Research and Isotope production General Atomics) Mark II is a research reactor designed and manufactured by General Atomics. It consists in a pool-type reactor cooled and partially moderated by light water through natural circulation, its fuel is characterized by a uniform mixture of uranium (8%wt, enriched at 20%wt in 235U) and zirconium hydride (ZrH), which provides neutron moderation inside the fuel itself [1]. This particular composition exhibits a large, prompt negative thermal coefficient of reactivity, which implies that in case the core temperature rises, the reactivity quickly reduces. This singular feature guarantees the characteristic inherent safety of the system. The TRIGA Mark II reactor installed at the University of Pavia is able to operate at 250 kW in full power and steady state conditions. The core is shaped like a cylinder with the fuel elements distributed along five concentric rings. Three control rods are employed to manage the core reactivity: SHIM, Regulating (REG) and Transient (TRANS). The core layout is displayed in Fig.1 . The reactor achieved its first criticality in 1965 and since then it has been exploited for several purposes such as the production of radioisotopes, nuclear activation analysis and development of boron neutron capture therapy in the medical field and reactor physics studies.

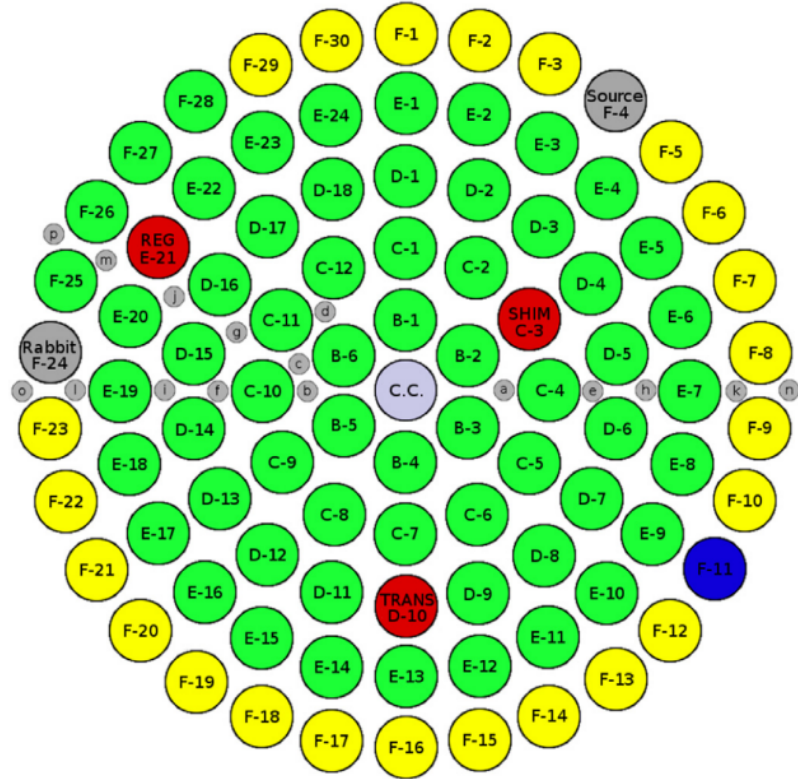


Figure 1: TRIGA's first configuration: fuel elements are represented in green, graphite rods in yellow, control rods in red and the empty slot in blue. The Central Channel is labeled with C.C. The smaller gray circles represent the holes found on the top core grid.

## 2. Objective

In this framework, a complete 3-D Monte Carlo model for neutronics was developed to simulate the reactor configuration at the first startup (1965), characterized by fresh fuel and zero power (10 W). This is the reactor's simplest conformation because the fuel is not heavily contaminated with fission reaction products and its original composition is known. Moreover, at zero power the fuel can be considered in thermal equilibrium with the water of the pool and, thus, can be considered at room temperature.

The objective is to simulate the neutrons' behavior inside the reactor, ignoring the thermal-hydraulics feedback and the time evolution of the system, in order to evaluate several parameters and compare them with the corresponding experimental values. The investigated factors are the two-group homogenized constants, the effective delayed neutron fraction  $\beta_{eff}$ , the calibration curve of the control rod REG, the fuel temperature prompt reactivity feedback  $\alpha_{T_{fuel}}$  and the void one  $\alpha_{void}$ .

### 3. Monte Carlo method and Serpent code

Generally, Monte Carlo method is a numerical technique that exploits the sampling of random values from a probability distribution in order to solve a problem. When dealing with neutron transport, this method simulates the stochastic trajectories of a set of particles. The larger the number of samples, the more accurate the result. In order to obtain the length of the particle path between two consecutive interactions, a probability density function is defined. This quantity represents the probability per unit length of such an event, so it is related to the total macroscopic cross section of the medium. Once the collision location has been identified, the code samples other random numbers to select the kind of interaction (scattering, capture, fission...) and the energy and angular variation of the neutron. This step sequence is repeated for each particle until it exits the domain or undergoes absorption.

The neutron population will grow or drop exponentially according to the multiplication factor  $k$ . Thus, simulating the path of all the neutrons becomes unpractical due to the increased demand for computational effort. To overcome this issue, Criticality calculations can be exploited. In these simulations the total number of particles is fixed regardless of the value of the multiplication factor, which is computed at each population's cycle, generation [2].

Differently from deterministic approaches, which provide exact solutions of approximated models, Monte Carlo one yields uncertain solutions to exact problems, despite they require significant time to reach a reliable result. In this context, Serpent is a multi-purpose three-dimensional continuous-energy Monte Carlo code for neutron and photon transport, developed at VTT Technical Research Centre of Finland since 2004. Neutron interaction physics in Serpent is based on classical collision kinematics and ENDF reaction laws. Cross sections are read from ACE format data libraries, which are pre-processed to a specific temperature and can be further adjusted to consider Doppler broadening effect or thermal scattering law.

### 4. Model

The core geometry is represented in Fig.2. Its internal diameter measures 45.7 cm and is surrounded by a graphite reflector of 80 cm outer diameter. Fuel elements are enclosed both on top and on bottom by 50 cm of water. As it can be seen, the system lacks symmetry, therefore it needs to be simulated entirely since no simplifications of this kind are allowed.

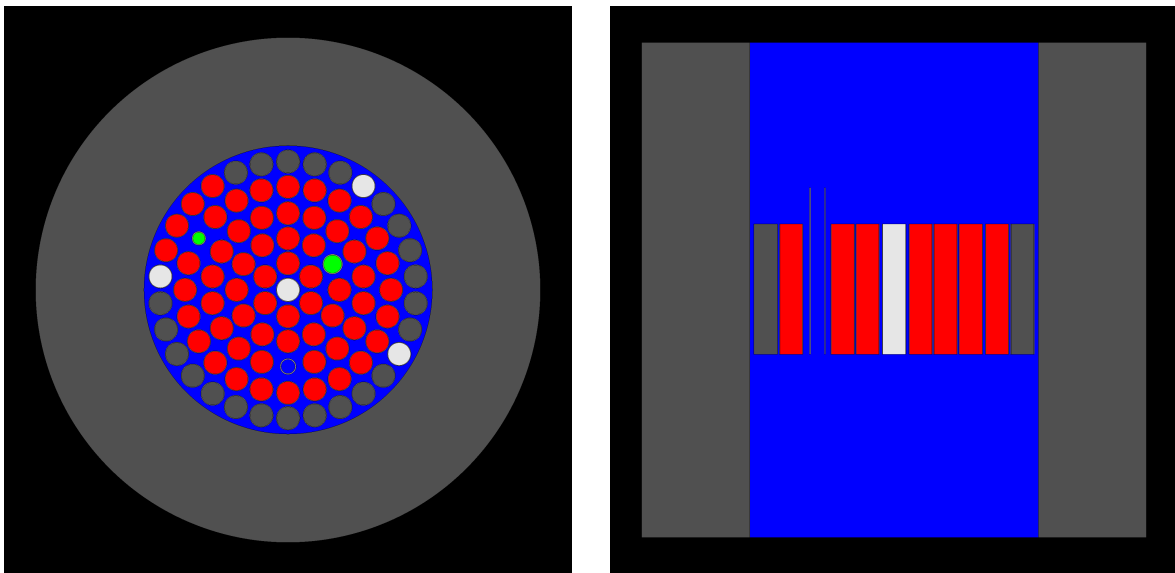


Figure 2: Horizontal (left) and vertical (right) cross sections of the core

The five concentric rings are placed respectively at 4.2, 8.15, 12.15, 16.33, 20.34 cm radially from the center. The core is composed by 61 fuel elements (red), 4 vacuum channels (white), 3 control rods (green), although TRANS isn't visible since it is completely withdrawn, and 23 graphite rods (grey).

The fuel and control rods' geometries are shown in Fig.3 and described in Tab.1 and Tab.2; while their compositions are listed in Tab.3 and Tab.4.

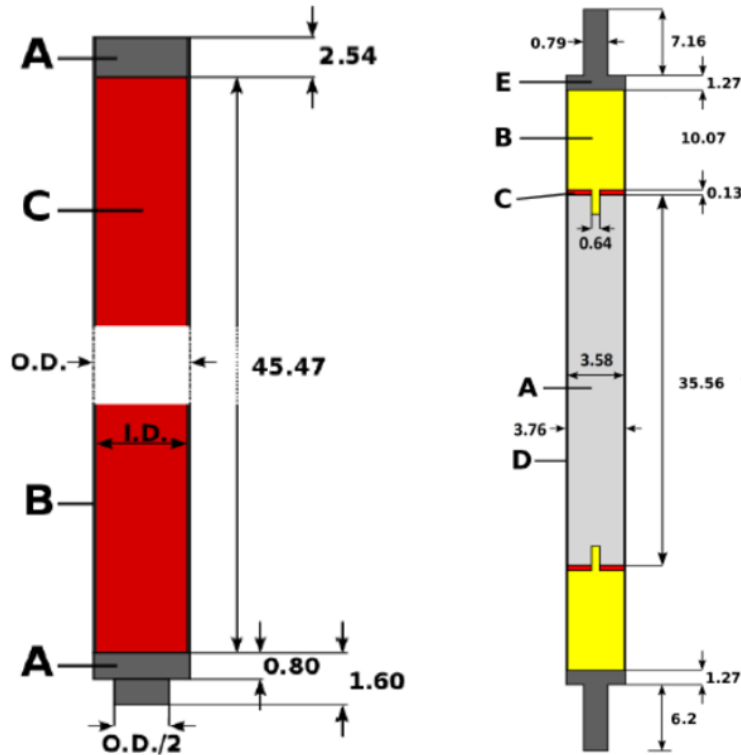


Figure 3: Fuel element (right) and control rods (left) geometries. Dimensions are reported in centimeters

| Control rods | Inner diameter (cm) | Outer diameter (cm)        |
|--------------|---------------------|----------------------------|
| SHIM         | 2.85                | 3.18                       |
| REG          | 1.93                | 2.22                       |
| TRANS        | 2.21                | 2.54                       |
| A            | Aluminum plug       | Neglected in Serpent input |
| B            | Cladding            | Aluminum alloy             |
| C            | Absorbing material  | $B_4C$                     |

Table 1: Control rods geometry

| Fuel elements |                                    |                            |
|---------------|------------------------------------|----------------------------|
| A             | Fuel                               | $UZr_1H_1$                 |
| B             | Axial neutron reflector (graphite) | Neglected in Serpent input |
| C             | Burnable poison disks (Samarium)   | Neglected in Serpent input |
| D             | Cladding                           | Aluminum alloy             |
| E             | Plug                               | Neglected in Serpent input |

Table 2: Fuel elements geometry

The simulation consists of 100 inactive cycles, used to allow the fission source to converge from the initial guess to its fundamental mode before the collection of the results, and 200 active cycles, during which the outcomes

| Control rods (Boron Carbide $B_4C$ ), density $2.52 \text{ g cm}^{-3}$ |                            |
|--|----------------------------|
| <i>Isotope</i>   | <i>Atomic fraction (%)</i> |
| C  | 20                         |
| $^{10}\text{B}$  | 15.8                       |
| $^{11}\text{B}$  | 64.2                       |

Table 3: Control rods composition

| Fuel elements (Uranium Zirconium Hydride $UZr_1H_1$ ), density $6.3 \text{ g cm}^{-3}$ |                          |
|--|--------------------------|
| <i>Isotope</i>   | <i>Mass fraction (%)</i> |
| H  | 1                        |
| Zr   | 91                       |
| $^{235}\text{U}$   | 1.6                      |
| $^{238}\text{U}$   | 6.4                      |

Table 4: Fuel elements composition

are truly acquired. The number of neutrons per cycle is 10000, although in certain cases it has been increased to improve statistics and lower the uncertainty.

Throughout the whole analysis, TRANS control rod was always completely lifted up, as done in reality in order to meet the safety guidelines, whereas SHIM was kept at 20 cm from the bottom of the core. REG instead was shifted at various heights to evaluate its calibration curve.

All the investigations discussed from now on, except for the calibration, were performed keeping REG totally inserted and at environmental temperature.

## 5. Results

### 5.1. Neutron flux spectrum

The reactor average neutron flux was estimated and its energy spectrum is shown in Fig.4 together with the ones in each of the core main components.

As expected, fast neutrons are more abundant inside the fuel, where they are created. REG and SHIM values have been increased by a factor of 100 to make them visible and, due to their high absorbing capacity, the thermal flux within them is close to zero. The reflector shows a large amount of low-energy neutrons, this happens because it moderates a great number of them within its large volume while they escape from the more internal part of the core. Water, instead, shows a greater amount of thermal neutrons than the fuel because the former is mostly just a source of moderation, while the latter is an effective absorber as well.

In general, without any doubt, the further the neutrons travel, the more energy they lose.

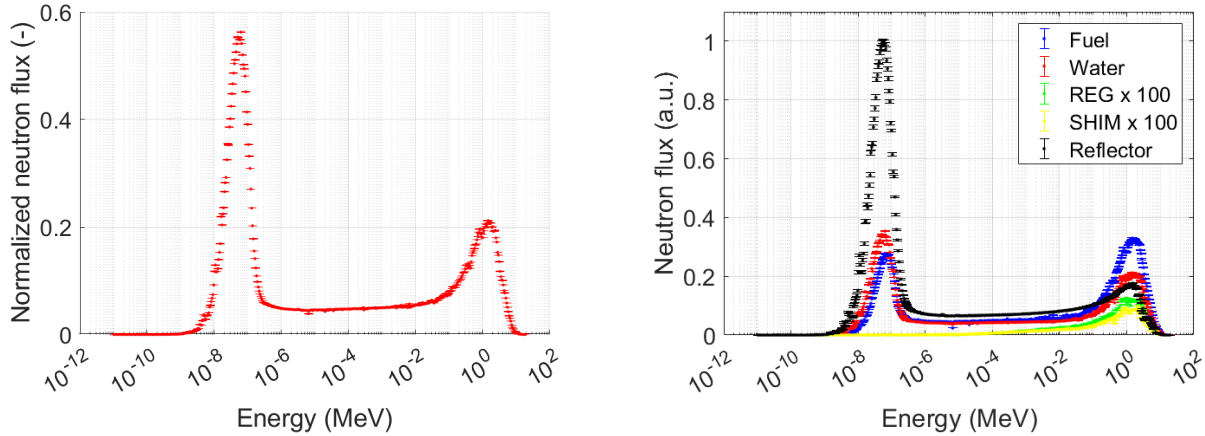


Figure 4: Normalized average neutron flux in the whole core (left) and inside its main components (right)

In Fig.5 it can be observed that most of the power is generated in the center, where the flux is higher and so is the number of fissions as well. A dark spot is also visible where REG is located, this is due to its high absorbing capacity, especially for thermal energies.

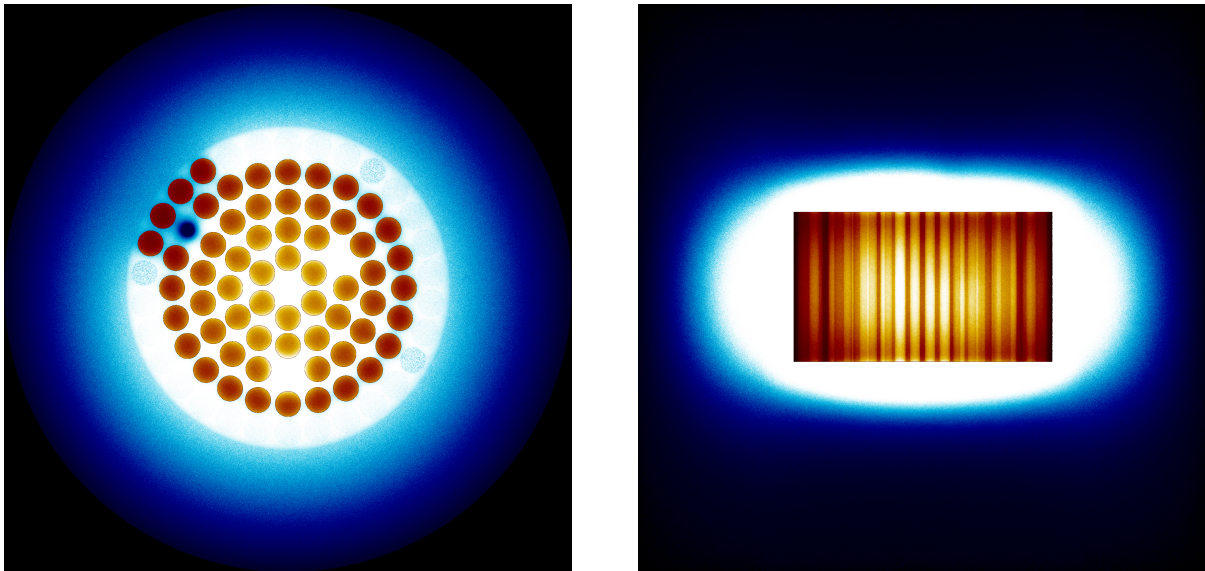


Figure 5: Fission power (hot color map) and thermal flux (cold color map)

In Fig.6 also the elastic, capture and fission rates in the internal side of the core are displayed. As it appears, water is clearly the medium where most of the scattering reaction occurs, followed by the fuel, where the high content of hydrogen supports neutrons moderation.

Regarding capture rate instead, the control rods are evidently the main contributors. It is also visible that, close to the fuels' periphery, the capture rate is larger. This phenomenon is due to the self-shielding effect: fission-generated neutrons exiting the fuel are scattered back by water and, since now their energy is lower, they are likely absorbed in the first zones they encounter on the way back. This leads to a much larger capture and fission rate, and so fuel consumption as well, close to the rod's periphery.

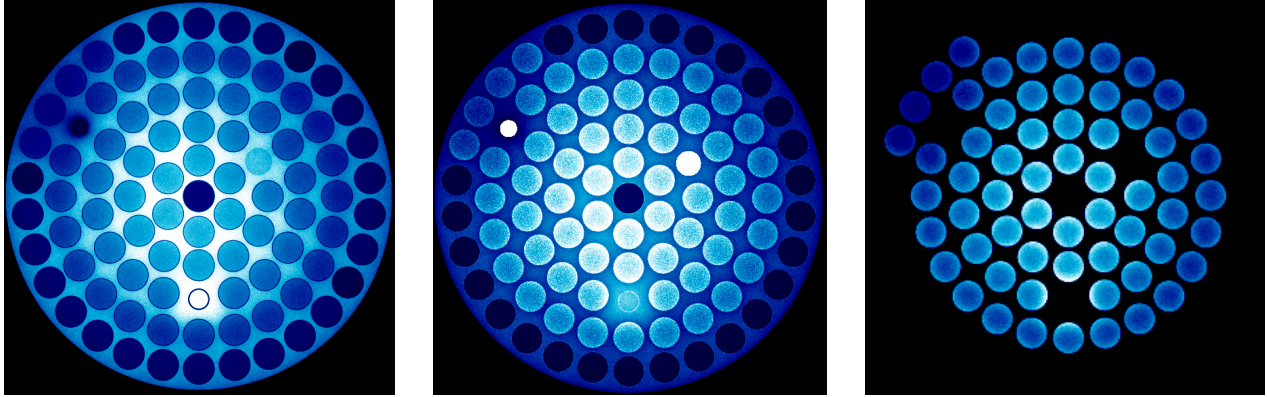


Figure 6: Cold color maps of elastic scattering (left), capture (center) and fission (right) reaction rates

## 5.2. Diffusion homogenized group constants

In this section are presented the numerical results of some group constants within the main materials of the core, useful to perform a two-group diffusion deterministic analysis of the TRIGA. The energy threshold was set at 0.625 eV. Group constants  $F$  are defined as the weighted average of the examined factor  $f$  by the neutron flux  $\phi$  in the selected volume and energetic field:

$$F_{i+1} = \frac{\int_{E_{i+1}}^{E_i} \int \phi(r, E) f(r, E) dV dE}{\int \int_{E_{i+1}}^{E_i} \phi(r, E) dV dE} \quad (1)$$

### 5.2.1 Two-group diffusion coefficients

An evaluation of the two-group diffusion coefficients was carried out. As it can be seen in Tab.5, the lowest values are found in the control rods, where the high probability of being absorbed makes it difficult for the neutron to travel long distances inside them.

| Diffusion coefficients (cm) | $D_{th} \pm 2\sigma$          | $D_f \pm 2\sigma$            |
|-----------------------------|-------------------------------|------------------------------|
| Fuel                        | $0.275 \pm 5 \times 10^{-5}$  | $1.159 \pm 4 \times 10^{-4}$ |
| Water                       | $0.159 \pm 2 \times 10^{-5}$  | $1.379 \pm 7 \times 10^{-4}$ |
| SHIM                        | $0.0088 \pm 9 \times 10^{-5}$ | $0.894 \pm 0.003$            |
| REG                         | $0.0086 \pm 6 \times 10^{-5}$ | $0.871 \pm 0.003$            |
| Graphite                    | $0.699 \pm 9 \times 10^{-5}$  | $1.004 \pm 5 \times 10^{-4}$ |

Table 5: Two-group diffusion coefficients for different materials

It can also be noticed that diffusion of fast neutrons is promoted, due to their higher kinetic energy and consequent lower absorption cross section.

### 5.2.2 Two-group macroscopic cross sections

Furthermore, an estimation of the absorption, scattering and fission macroscopic cross-sections of the different materials was conducted taking into account a two-group approximation. Their values are presented respectively in Tab.6, Tab.7, Tab.8.

These values are in agreement with the previous plots concerning reaction rates.

Reasonably, SHIM and REG absorption capabilities are significantly larger with respect to other components. This is mostly due to the presence of  $^{10}B$ , which exhibits a remarkably large absorption cross-section, especially in the thermal region. Scattering instead is promoted in the fuel and water, where hydrogen is abundant. Overall it is clear that neutron-nuclei interactions are favored in the thermal group, given that cross-sections of the considered isotopes are larger at lower energies.

| Absorption cross sections ( $\text{cm}^{-1}$ ) | $\Sigma_{th}^a \pm 2\sigma$               | $\Sigma_f^a \pm 2\sigma$                   |
|--|---|--|
| Fuel   | $0.1292 \pm 1 \times 10^{-5}$             | $0.0074 \pm 3 \times 10^{-6}$              |
| Water  | $0.0175 \pm 9 \times 10^{-7}$             | $4.31 \times 10^{-4} \pm 1 \times 10^{-7}$ |
| SHIM   | $46.53 \pm 0.07$                          | $0.1616 \pm 4 \times 10^{-4}$              |
| REG  | $47.50 \pm 0.05$                          | $0.212 \pm 8 \times 10^{-4}$               |
| Graphite                                       | $2.9 \times 10^{-4} \pm 5 \times 10^{-8}$ | $2.6 \times 10^{-5} \pm 1 \times 10^{-7}$  |

Table 6: Two-group macroscopic absorption cross sections for different materials

| Scattering cross sections ( $\text{cm}^{-1}$ ) | $\Sigma_{th}^s \pm 2\sigma$  | $\Sigma_f^s \pm 2\sigma$     |
|--|------------------------------|------------------------------|
| Fuel   | $1.722 \pm 1 \times 10^{-4}$ | $0.688 \pm 5 \times 10^{-5}$ |
| Water  | $3.087 \pm 9 \times 10^{-5}$ | $0.924 \pm 9 \times 10^{-5}$ |
| SHIM   | $0.615 \pm 0.092$            | $0.442 \pm 7 \times 10^{-4}$ |
| REG  | $0.615 \pm 0.069$            | $0.449 \pm 0.001$            |
| Graphite                                       | $0.483 \pm 1 \times 10^{-5}$ | $0.407 \pm 4 \times 10^{-5}$ |

Table 7: Two-group macroscopic scattering cross sections for different materials

| Fission cross sections ( $\text{cm}^{-1}$ ) | $\Sigma_{th}^{fis} \pm 2\sigma$ | $\Sigma_f^{fis} \pm 2\sigma$  |
|---|---------------------------------|-------------------------------|
| Fuel  | $0.0974 \pm 9 \times 10^{-6}$   | $0.0024 \pm 5 \times 10^{-7}$ |

Table 8: Two-group macroscopic fission cross sections for different materials

## 6. Comparison with experimental results

### 6.1. Effective delayed neutron fraction

The first outcome validation of the reactor model involved the evaluation of the effective fraction of delayed neutrons  $\beta_{eff}$  over the total number of neutrons generated in the fission process. In fact, given that delayed neutrons are emitted typically at lower energies than fission ones (400 keV against 2 MeV) and since inside a thermal reactor the fission chain is sustained mainly by thermal neutrons, their probability of fissioning a nucleus is higher. This is the reason why  $\beta_{eff}$  is larger than its corresponding theoretical value:  $\beta = 650 \text{ pcm}$  for  $^{235}\text{U}$ .

The formal definition of  $\beta_{eff}$  is reported in Eq.2. The main obstacle to its resolution is the estimation of the adjoint flux  $\phi^+$ .

To perform the calculation with Serpent, Meulekamp's method was exploited, which essentially states that  $\beta_{eff}$  is given by the ratio between the number of fissions generated just by delayed neutrons and their total amount.

$$\beta_{eff} = \frac{\int \int \int \phi^+(r, E, \Omega) \chi_d(E) \nu_d(E) \Sigma_f(r, E) \phi(r, E, \Omega) dV dE d\Omega}{\int \int \int \phi^+(r, E, \Omega) \chi(E) \nu(E) \Sigma_f(r, E) \phi(r, E, \Omega) dV dE d\Omega} \quad (2)$$

A comparison with the value calculated using the k-ratio method [3], displayed in Eq.3, where  $k_\rho$  is the multiplication factor obtained considering just fission neutrons and  $k_t$  including also delayed ones, is presented in Tab.9.

$$\beta_{eff} = \frac{k_t - k_\rho}{k_t} \quad (3)$$

The two values are close to each other: the model concurs with the experimental result, indicating its trustworthiness.

| Effective delayed neutron fraction (pcm) | $\beta_{eff} \pm 2\sigma$ |
|--|---------------------------|
| Serpent model                            | $757.72 \pm 11.18$        |
| k-ratio method [4]                       | 730                       |

Table 9: Effective delayed neutron fraction comparison

## 6.2. REG control rod worth

The change in reactivity caused by the movement of a control rod from its out-core position to its complete insertion is called control rod worth and is a key parameter to manage the reactor. Its assessment for REG through Serpent code has been carried out simply by taking the difference between the core reactivity when REG was completely lifted and inserted, as done in Eq.4.

$$\Delta\rho_{REG} = \rho_{REG_{out}} - \rho_{REG_{in}} \quad (4)$$

The result is shown in Tab.10 and it is compared with the experimental ones measured in 1965, when TRIGA began operation, by LENA [5] and in 2023 through the reactor period method with the academic course *Experimental Nuclear Reactor Kinetics* held by Prof. Lorenzi at Politecnico di Milano, which from now on will be labeled as ENRK experiment. A fundamental detail that needs to be clarified is that in 2013 TRIGA's configuration was changed (as shown in Fig.7), essentially increasing the number of fuel elements in order to reach the full power of 250 kW and to extend its operational life. This means that ENRK experiments were taken on a different core design, so the hypothetical difference between their outcomes and Serpent ones needs to be interpreted.

| REG control rod worth (\$) | $\Delta\rho_{REG} \pm 2\sigma$ |
|----------------------------|--------------------------------|
| Serpent model              | $1.639 \pm 0.031$              |
| Experiment [5]             | $1.645 \pm 0.064$              |
| ENRK experiment            | $1.191 \pm 0.013$              |

Table 10: REG control rod worth comparison

Looking at the results, it can be observed that the model's outcome is much closer to the 1965 one than to the more recent one. This may be due to the fact that, in the new conformation, fuel elements have been put in place of all graphite rods. This leads to a more symmetric layout, therefore the neutron flux's peak is closer to the core center. In the original configuration instead fuel elements were arranged in an asymmetric disposition, therefore the neutron flux reached its maximum not in the middle, but slightly moved towards REG's location, where more fuel rods are placed. This is why REG's control rod worth is greater in the first design although it had less fuel: because flux in that position was proportionally higher (as shown in Fig.5).

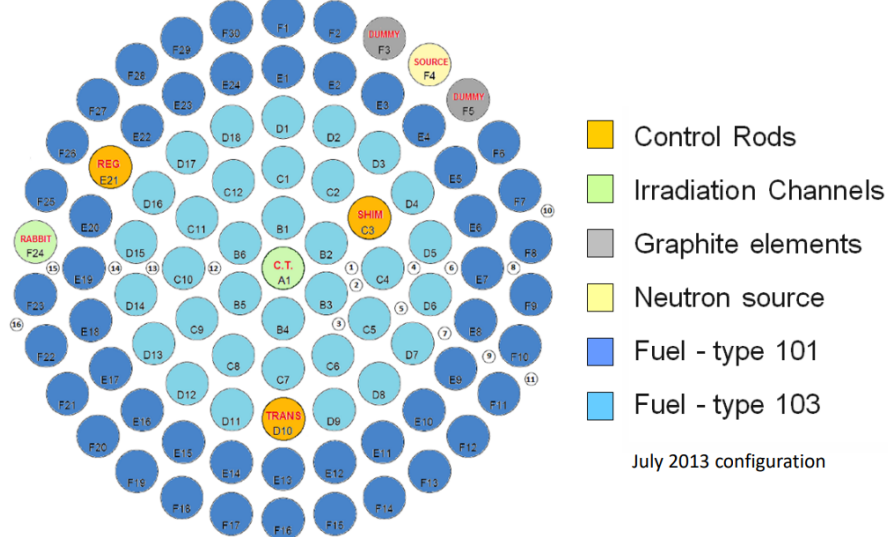


Figure 7: TRIGA’s new configuration

### 6.3. REG calibration curve

Control rod calibration is an important safety benchmark to determine the core excess and the shutdown margin based on its position. The REG calibration curve has been estimated by running the simulation with different REG height positions and computing each time the difference between the current core reactivity level and the one when the control rod was totally inserted, as in Eq.5.

$$\Delta\rho(z) = \rho(z) - \rho_{REG_{in}} \quad (5)$$

The obtained outcome is displayed in Fig.8 along with the experimental ones acquired in 1965 [5] and 2023.

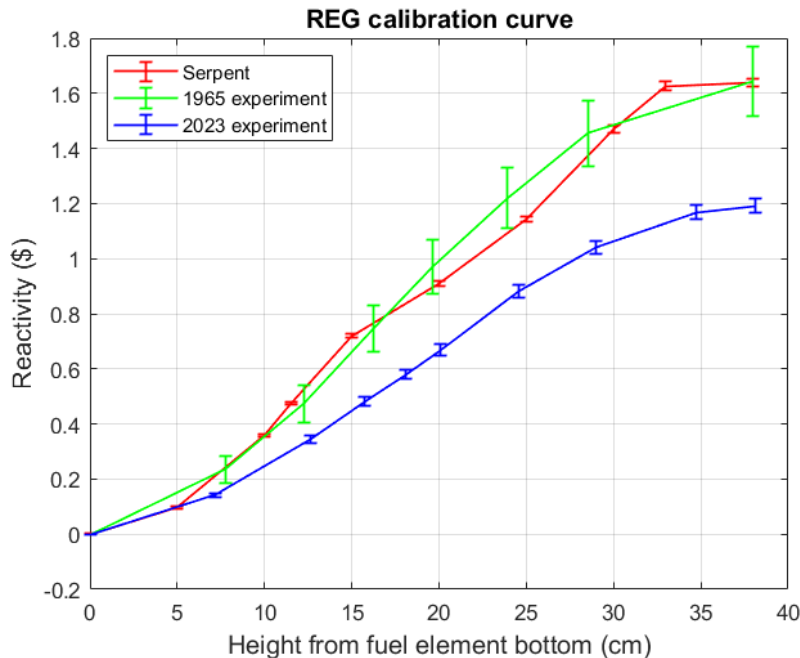


Figure 8: REG calibration curve and 95% confidence interval

All three of them exhibit a trend that resembles a sinusoidal function, as we would expect, and the slope is maximum at half height, where the neutron flux is higher and so the absorbing effect is enhanced. The simulated results again agree much more with 1965’s ones for the same above-mentioned reasons.

## 6.4. Fuel temperature prompt reactivity coefficient

When the fuel temperature changes, it carries to a prompt reactivity variation by means of a few major mechanisms: Doppler and spectral hardening effects. Doppler broadening of cross sections in the resonance region increases the probability for a neutron to be captured while moderated. The thermal motion of the target nucleus,  $^{238}U$  in particular, widens the energy interval of acceptance of the resonance, improving the absorption rate. The consequence is that fewer neutrons are able to reach thermal energies, where fission is favored. This phenomenon is described by Eq.6, where  $I$  is the resonance integral and  $p$  is the resonance escape probability.

$$\alpha_{Doppler} = \frac{1}{p} \frac{\partial p}{\partial T_{fuel}} = \frac{1}{p} \frac{\partial p}{\partial I} \frac{\partial I}{\partial T_{fuel}} = \frac{1}{I} \frac{\partial I}{\partial T_{fuel}} \ln(p) \propto -\frac{1}{\sqrt{T_{fuel}}} \quad (6)$$

The spectral hardening phenomenon is due to the singular fuel composition. Differently from other thermal reactors, TRIGA employs  $UZr_1H_1$  as a fuel and the hydrogen inside of it contributes to moderation. However, its behavior becomes much different from that of free hydrogen, since it is bounded in a crystalline structure, at incident neutron energies below 0.137 eV. In this region neutrons are much less able to transfer their energy to the target and the upscattering process becomes significant, therefore further moderation within the fuel is hindered. This latter phenomenon is promoted at higher temperatures since the probability that a nucleus will occupy a more energetic state is enhanced. The spectral hardening leads to larger leakage probability and lower average absorption cross sections in the fuel pellet, heading to a reactivity decrease.

To evaluate the influence of these two contributions, a uniform fuel temperature increase of 50 °C was considered. Two simulations were made: first, in order that the change of temperature acted only on the Doppler broadening of cross sections, the thermal library of hydrogen wasn't altered; in a second moment instead, the one at 50°C more was taken.

The procedure to estimate the reactivity effect is described in Eq.7.

$$\alpha_{T_f} = \frac{\partial \rho}{\partial T_{fuel}} \approx \frac{\rho_{T_{hot}} - \rho_{T_{room}}}{T_{hot} - T_{room}} \quad (7)$$

Results are compared with experimental ones in Tab.11. As it was expected, Doppler contribution is around 30% of the total reactivity coefficient [3], meaning that the main contribution is due to spectral hardening, characteristic of TRIGA's fuel.

| Fuel temperature prompt reactivity coefficient ( $\frac{pcm}{K}$ ) | $\alpha_{Doppler} \pm 2\sigma$ | $\alpha_{T_{fuel}} \pm 2\sigma$ |
|--|--------------------------------|---------------------------------|
| Serpent model  | -1.970 ± 1.078                 | -7.782 ± 1.049                  |
| Experiment [6]   | -2.6 ± 0.5                     | -8.6 ± 0.5                      |
| ENRK experiment  | -                              | -10.577 ± 3.252                 |

Table 11: Fuel temperature prompt reactivity coefficient comparison

As expected, values are largely negative, this means that, following a rise of fuel temperature, the reactivity would rapidly drop, stabilizing the reactor operation.

## 6.5. Void reactivity coefficient

In case a void is generated in the core, the moderator volume decreases, leading to an increase in two competitive phenomena: thermalization and capture, which were enhanced by the higher moderator density. This suggests that void creation may lead to a rise or reduction of reactivity depending on which mechanism prevails on the other one. An example of a cause for void production is subcooled boiling.

TRIGA is designed to have a negative void reactivity. In the Serpent simulation, the evaluation was conducted by simply filling the central channel with water and computing the obtained  $k_{eff}$ . Then the reactivity variation with respect to the initial void-filled case was calculated and divided by the moderator volume change, as in Eq.8.

$$\alpha_{void} = \frac{\partial \rho}{\partial V} = -\frac{\partial \rho}{\partial V_{water}} \approx -\frac{\rho_{water} - \rho_{void}}{V_{water}} \quad (8)$$

Serpent and experimental results are shown in Tab.12.

| Void reactivity coefficient ( $\frac{pcm}{cm^3}$ ) | $\alpha_{void} \pm 2\sigma$ |
|--|-----------------------------|
| Serpent model                                      | -0.419 $\pm$ 0.201          |
| Experiment [7]                                     | -0.3 $\pm$ 0.1              |
| ENRK experiment                                    | -0.153 $\pm$ 0.391          |

Table 12: Void reactivity coefficient comparison

The obtained values are negative, this implies that void creation leads to reactivity reduction, since the major contribution of water is related to neutron moderation, therefore an increase of void would generate negative feedback on core reactivity.

## 7. Conclusion

To summarize, for the most part, the data calculated through Serpent shows a good agreement with the experimental results. Therefore, the accordance between these two validates the reliability and accuracy of the developed model. A further improvement would be to implement the components ignored in this first analysis and increase the number of cycles and neutrons simulated, although this would negatively affect the already demanding computational cost, and so the required time, for the simulation.

Thanks for reading.

## References

- [1] Cammi A. Zanetti M. *Characterization of the TRIGA Mark II reactor full-power steady state*. 2015.
- [2] Boccelli R. *Numerical evaluation of reactivity feedback coefficients in TRIGA mark II reactor through a Monte Carlo approach*. 2022.
- [3] Comision Nacional de Energia Nuclear de Mexico. *Kinetic behavior of TRIGA reactor*. 1967.
- [4] Borio Di Tiglione A. Cammi A. *Benchmark evaluation of reactor critical parameters and neutron fluxes distributions at zero power for the TRIGA Mark II reactor of the University of Pavia using the Monte Carlo code MCNP*. 2010.
- [5] L.E.N.A. *Calibrazione finale delle barre di controllo*. 1965.
- [6] S. Boarin A. Cammi M.E. Ricotti D. Chiesa M. Nastasi E. Previtali M. Sisti G. Maggiori M. Prata A. Salvini. *Setting-up a control-oriented model for simulation of triga mark ii dynamic response*. 2018.
- [7] L.E.N.A. *Specifica tecnica della prova relativa al coefficiente di vuoto della reattività in varie posizioni del noccioleto*. 1965.